Alaa Hasan
Department of Mechanical Engineering,
University of Wisconsin-Milwaukee,
115 East, Reindl Way,
Glendale, WI 53212
e-mail: mahmoud9@uwm.edu

Abdel Rahman Salem
Department of Mechanical Engineering,
University of Wisconsin-Milwaukee,
115 East, Reindl Way,
Glendale, WI 53212
e-mail: assalem@uwm.edu

Ahmad Abdel Hadi
Department of Mechanical Engineering,
University of Wisconsin-Milwaukee,
115 East, Reindl Way,
Glendale, WI 53212
e-mail: aiajr@uwm.edu

Mohammad Qandil
Department of Mechanical Engineering,
University of Wisconsin-Milwaukee,
115 East, Reindl Way,
Glendale, WI 53212
e-mail: mdqandil@uwm.edu

Ryoichi S. Amano[1]
Fellow ASME
Department of Mechanical Engineering,
University of Wisconsin-Milwaukee,
115 East, Reindl Way,
Glendale, WI 53212
e-mail: amano@uwm.edu

Ammar Alkhalidi
Department of Energy Engineering,
German Jordanian University,
Amman 11180, Jordan
e-mail: ammar.alkhalidi@gju.edu.jo

The Power Reclamation of Utilizing Micro-Hydro Turbines in the Aeration Basins of Wastewater Treatment Plants

Upgrading the aeration basin technology can improve the oxygen transfer efficiency (OTE), while keeping the energy consumption at its minimum level. Therefore, this paper introduces a new idea of installing micro-propeller turbines in the aeration basin of a wastewater treatment plant (WWTP) to extract power from the high-velocity location in the water column. This extracted power can be used to operate a mixer at the top of the membrane to induce the mixing in that region, which will drive the less oxygenated wastewater into the water column. The rest of the extracted power will rotate microturbine rotors for electric power generation. By applying the proposed microturbines to the 13 audited facilities, it was demonstrated to achieve a gross annual energy-savings of 3,836.9 MWh, a gross annual cost-saving of $260,497, and total CO_2 emissions that would be reduced by 2,714 metric tons/year. Generally, the addition of the proposed microturbines can save up to 15.7% of the annual plant electricity consumption (1.3–12.8% of the plant annual electricity bills). [DOI: 10.1115/1.4048869]*

Keywords: wastewater treatment plants, aeration basins, energy efficiency, power reclamation, micro-propeller turbine, alternative energy sources, energy conversion/ systems, energy systems analysis, renewable energy

Introduction

Within the last few decades, energy-saving [1], renewables development [2–4], and resource recovery [5] have become a goal for plants and utilities throughout the world. Therefore, energy audit-related papers analyzed the energy usage and monthly energy cost for various applications: wastewater treatment plants (WWTPs), iron and steel forgings, aluminum die-casting, commercial printing, and plastic production facilities. A considerable reduction in energy usage of motors, compressed air systems, lighting, and pumps was achieved by the participated facilities. WWTPs showed high energy-saving possibilities, among other facilities [6–8].

Because of the high energy-saving potential in WWTPs, Nourin et al. discussed the economic and environmental aspects of installing a combined heat and power (CHP) system at many WWTPs. The study introduced the benefits of using a micro-gas turbine (MGT) to drive absorption chiller for the WWTPs [9].

Wastewater treatment plants across the United States face challenges of growing hydraulic demand, rising operating costs, an increase in regulatory requirements, and outdated equipment and facilities. Throughout the country, cost cut is always an ultimate goal for treatment plants, while improving effluent quality and meeting temperature standards should be achieved simultaneously. In the US around 35% of the typical municipal energy budget is for the water and WWTPs. The WWTPs consume about 4% of the total energy consumption in the US each year. Because treatment plants require significant energy input, energy efficiency offers an expanding opportunity to trim operating costs [10,11].

The first step to reducing energy consumption and lower the cost of power generation is improving energy efficiency, and that helps in reaching the main goal to counter the increase in energy use at WWTPs [12]. Two important factors must be analyzed for many of the methods used to achieve energy neutrality explicitly. Water waste standards must be maintained, while the additional capital cost for modification of equipment in wastewater treatment plants must be accepted by plant owners. Consequently, most research always strives to promote energy balance and improve the relationship between wastewater quality and energy cost [13].

The treatment of wastewater is mainly incorporated into two stages. First, the wastewater flows through a filtration process
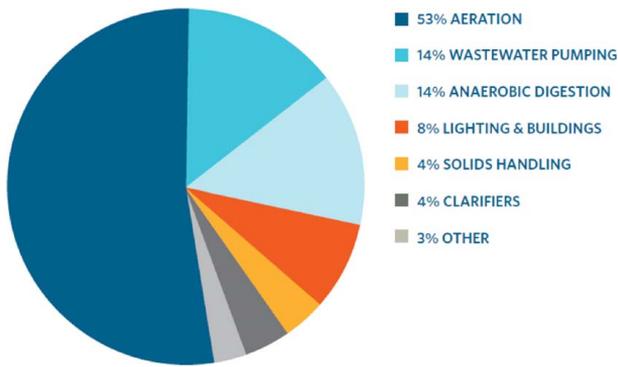
Fig. 1 Typical WWTP energy use distribution [14]

- 53% AERATION
- 14% WASTEWATER PUMPING
- 14% ANAEROBIC DIGESTION
- 8% LIGHTING & BUILDINGS
- 4% SOLIDS HANDLING
- 4% CLARIFIERS
- 3% OTHER

using screens of different sizes. This is called the primary treatment stage, where larger particles are removed from the wastewater. Suspended and dissolved particles are removed from the wastewater during the second stage. In the secondary treatment, the wastewater is admitted to the aeration tank, where it will be brought to contact with air.

In a typical WWTP, the aeration system uses between 40% and 60% of the plant's total energy consumption (see Fig. 1). Nationwide, more than $4 billion are spent annually on WWTPs' electrical bills. Therefore, any minimal energy-saving or energy-reclamation solution is considered a significant reduction in the energy costs of municipalities across the country.

Upgrading the aeration basin technology can improve the oxygen transfer efficiency (OTE) while keeping the aeration blower's energy consumption at its lowest possible level. The improvement can be achieved by upgrading from coarse bubble diffusion to fine bubble diffusion to increase the OTE and reduce blower load while maintaining proper dissolved oxygen (DO) control. Reducing aeration power can also be achieved by installing automated DO controls to reduce aeration energy by up to 40% compared to control systems that use manual sampling. Since systems that rely on manual DO sampling often operate at DO levels that are much higher than necessary, installing a DO sensor with integrated aeration control allows levels to be maintained within a narrower range, thereby reducing blower load. Furthermore, adding DO probes to different zones of the aeration basin provides more accurate DO readings and optimized aeration for each zone [14,15].

Alkhalidi and coauthors investigated the factors that affect very small-sized bubble creation and its size in a wastewater treatment
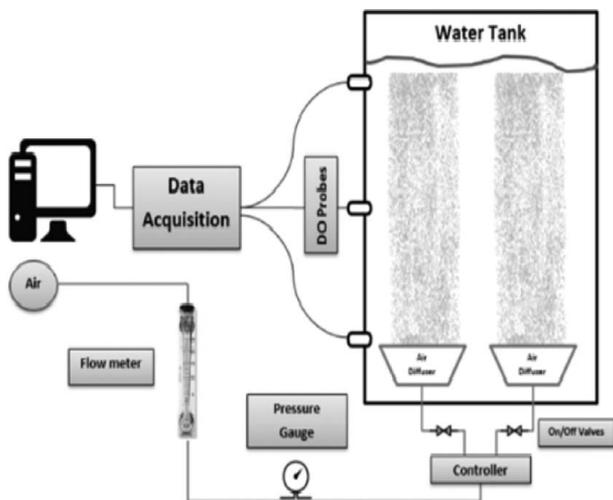
system using both computational fluid dynamics (CFD) and experimental techniques [16,17]. Among the airflow rate, inlet pressure, and contact angle for the rubber membrane, the flowrate had the most substantial effect on the bubble size. Great attention should be paid to the flowrate per each punch to reduce the bubble size, since fine bubbles are desired because their surface area is larger, and they stay longer through water, hence improving the standard oxygen transfer efficiency (SOTE), which will considerably improve the standard aeration efficiency (SAE). This could be achieved by increasing the number of punches in the diffuser membrane, which will reduce the flowrate per punch and increase the number of bubbles released in the water.

It has been proven in Refs. [18,19] that pulsating flow in the aeration system is more efficient than that of continuously compressed air (see Fig. 2). SOTE was studied at different column heights (0.6, 1.2, and 1.8 m), pulsating times (0.5, 1.5, and 2.5 s), and airflow rates (14–70 L/min). Airflow was supplied through a pressure gauge and a flowmeter and passed through diffusers that were connected with upstream solenoid valves after it passed a control circuit that acted as an off/on switch to create the pulsating effect. To measure the DO concentration, three probes were installed along with the water tank with 1-Hz frequency. DO concentrations obtained from these three probes were averaged to obtain the OTE. Those researchers found that the SOTE of the lowest pulsating time (0.5 s) exceeded the SOTE of the other pulsating times for all column heights, particularly at high flowrates. In general, the range of SOTE increased with the column height increase.

Amano and Alkhafaji [20] studied how the design parameters of ceramic diffusers can be influenced when considering different water columns and pulsating times. Aeration diffusers can be classified as fine and coarse diffusers based on the size of the diffuser holes. Fine pore diffusers generate fine bubbles that have been proven to transfer oxygen faster than coarse bubbles.

All the results were investigated for three water columns, 0.6, 1.2, and 1.8 m, and three pulsating times, 0.5, 1.5, and 2.5 s, while airflow rate ranged from 14 to 70 L/min. At 0.6-m column height, the ceramic diffusers gave better SOTE at lower flowrates (less than 40 L/min) than higher flowrates, for all pulsation times, except for 2.5 s, where the ceramic diffuser outperformed the membrane at all flowrates. For 1.2-m column height, ceramic diffusers showed negligible superiority over membrane at a pulsation time of 0.5 s, while the transcendence was considerable at 1.5 and 2.5 s. Finally, at 1.8-m column height, SOTE of the ceramic diffuser was better than the membrane for all pulsation times only at low flowrates (less than 30 L/min).

Al Ba'ba'a and Amano [21] investigated the effect of the orifice diameter, airflow rate, and the water column on the aeration efficiency. They used a single orifice in a cylindrical tank for air injection with 0.21–0.41 mm orifice diameters, under submergence heights of 0.46–0.91 m with airflow rates ranging from 0.05 to 0.125 standard liter per minute (SLPM). They monitored the DO concentration after the deoxygenation was completed. They tested 60 different combinations of orifice sizes, airflow rates, and water column heights. They found that the orifice diameter of 0.3 mm did better in testing under 0.69-m and 0.91-m immersion heights. A higher standard oxygen transfer rate (SOTR) was observed at deeper submergence due to a longer mass transfer duration with a greater concentration gradient. The highest aeration efficiency (SAE) was achieved at 0.3-mm orifice at 0.91-m immersion height with a 0.050 SLPM airflow rate. SAE is expected to decline significantly with an orifice diameter larger than 0.41 mm, due to inefficient oxygen mass transfer. The most parameters that affect the SAE are orifice diameter, airflow late, and then lastly followed by the water column due to their impact on the oxygen mass transfer coefficient and energy consumption.

To increase the OTE without increasing the power required to pump air into aeration tanks, Alkhaldi et al. [22] added a mixer and turbine blades to the regular fine bubble aeration diffuser. The turbine blade extracts power from the moving water current and transfers this power to the mixer at the top of the diffuser. A

Fig. 2 Pulsating jet experimental setup [18]
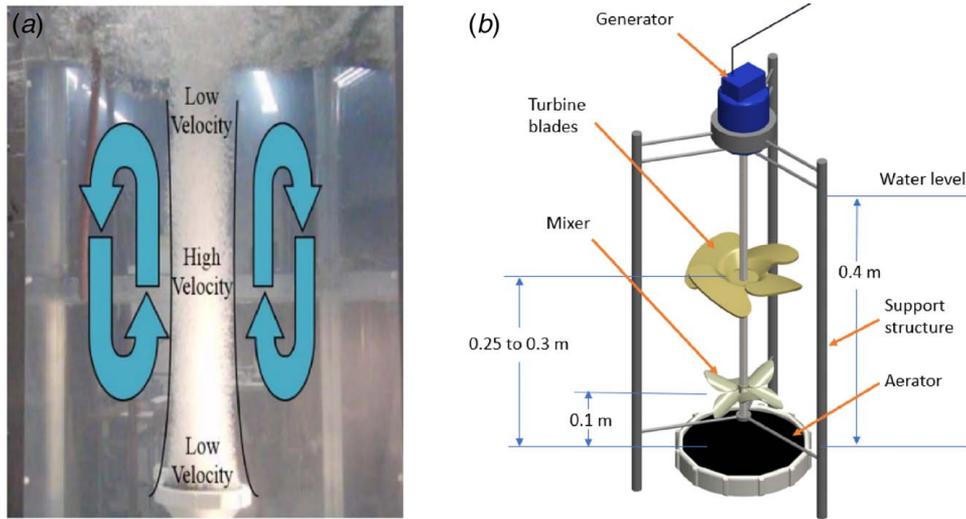
Fig. 3 (a) Bubble column details [22] and (b) computer-aided design (CAD) details of the experimental setup used on Ref. [22]

support structure was mounted above the air to connect the turbine blade and the mixer on one shaft. Moreover, they extracted the extra energy from the system at high flowrates using an electrical generator that was connected to the shaft. They used particle image velocimetry (PIV) to measure bubbles' velocity at different locations along the bubble column. It was found that the highest velocity is obtained in the middle of the column, while the lowest velocities were obtained just above the air diffuser and at the water surface. In their work, the energy was extracted from a high-velocity location in the water column and reutilized at the low-velocity location to improve OTE distribution. This was achieved by using an innovative self-powered mixer device located right above the membrane combined with a turbine blade at the highest velocity location. The use of the self-powered mixer indicated an increase in OTE of approximately 25% at high flowrates in the best cases using the sharp-nub (S–N) diffuser system. Moreover, results indicated a significant ability to reclaim the power of up to 11% of air pumping power, particularly at the highest flowrates.

The objective of this paper is to show the impact of implementing the proposed idea in Ref. [22] on all the thirteen WWTPs visited during the period from 2017 to 2020. Detailed calculations will be shown of the annual energy-savings, annual cost savings, implementation cost, payback periods, and the avoided CO_2 emissions that highlight the economic and environmental impact of the idea.

Methodology

Original Setup. According to Alkhalidi et al. [22], it was observed that when air is allowed through the diffusers installed at the bottom of an aeration tank, it develops a water-bubble current within the aeration pool (see Fig. 3(a)). This current is called the "bubble column" that was created by buoyancy force while driving bubbles toward the water surface. They used a clear plex-glass tank with the dimensions 0.9 m × 0.9 m × 1.2 m, while the water level was 0.4 m. By measuring the water velocity at different heights within the 0.4-m column using PIV, they noticed that water velocity culminated at around 63–75% of the water height. That is why they decided to install turbine blades and mixers to harness the high-velocity water current using the experimental setup whose computer-aided design (CAD) details are demonstrated in Fig. 3(b).

The water current is shown in Fig. 3(a), and the velocity profile is shown in Fig. 4(a), depicting that high kinetic energy exists in the middle of the bubble column and low energy at the lower end of the

column. Based on that observation, a new idea emerged to install a propeller turbine to extract power from the high-velocity location in the water column. A portion of this extracted power will be used to operate a mixer at the top of the membrane (low-velocity region) to induce the mixing in that region. The mixing of oxygen-water
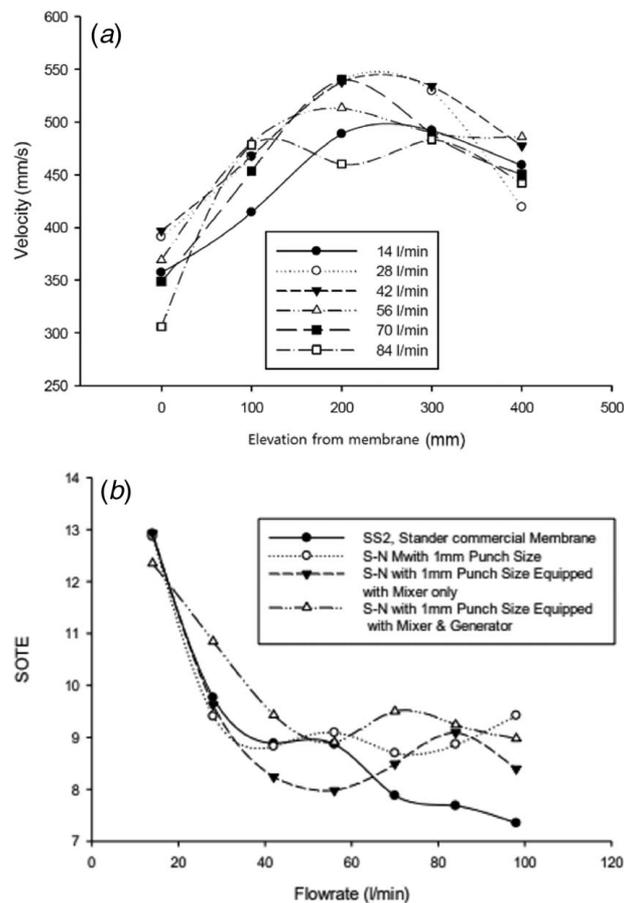
Fig. 4 (a) Water column velocity at different heights from the membrane at different flowrates [22] and (b) graphical illustration of resulting SOTE results for the standard membrane (SS2) compared to the S–N membrane [22]
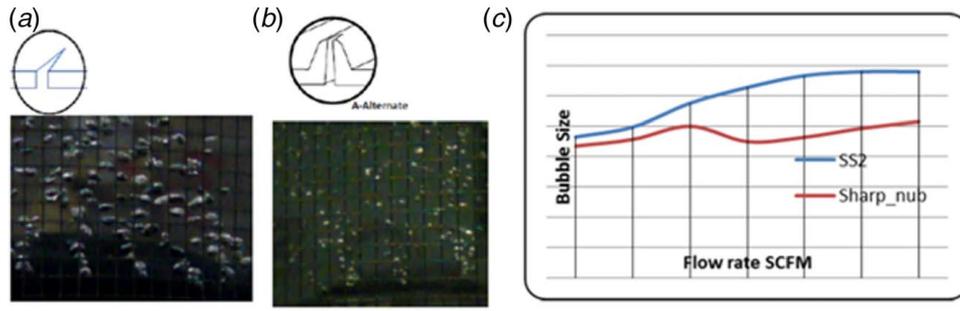
Fig. 5 Bubble size comparison between market aeration diffuser and sharp-nub diffuser [23]: (a) bubbles from a market aeration diffuser, (b) bubbles from a sharp-nub diffuser, and (c) bubble size difference. SS2-commercial diffuser, and sharp-nub orifice-hole diffuser.

drives less oxygenated wastewater into the water column. Therefore, the oxygen concentration difference between the inside and the outside of the air bubble will increase, and as a result, the SOTE will increase. The rest of the extracted power will rotate low revolutions per minute (rpm) generator above the water surface for electric power generation (see Fig. 3(b)).

The original turbine-mixer set by Alkhalidi had a drawback, which was a minimal decrease in the SOTE (15%) when the commercially standard membranes were used in the experimental aeration tank. However, SOTE increased when the original setup was used along with (S–N) membranes invented by Amano and Alkhalidi [23] (see Fig. 4(b)). S–N is a membrane that includes a nub with a perforation. The nub and perforation are arranged and sized to create smaller bubbles of air in the liquid column above the membrane. This effect is depicted in Fig. 5.

Proposed Setup. During the experiment at the University of Wisconsin-Milwaukee (UWM) aeration lab, the mixer was placed at 25% and turbine blades were placed 63% of the water level inside the tank. These percentages might be applied to all aeration tanks of the studied plants, but in situ verification of the high-velocity location is needed for real plant implementation. Turbine-mixer sets are proposed to be installed on a lateral basis along the aeration tank edges of the 13 WWTPs subjected to study in this work. The locations are chosen this way to make maintenance easier. The entire structure should be designed in a way that

permits pulling out the turbine from the dirty water to be fixed and then installing it again without emptying the tank.

Meanwhile, the proposed setup is shown in Fig. 6. The proposed installation heights are calculated based on an aeration tank depth of 3.81 m in one of the studied plants (with 3-m water level). In a typical WWTP, the standard polyvinyl chloride air diffuser's diameter is 0.23 m. Hence, the diameter of the proposed turbine should be 0.178 m, following the original setup done by Alkhalidi. Membranes and turbine parts should get a hydrophobic coat with a surface finish to resolve any scaling, particle, and algae interaction to help make it self-cleaning.

In the proposed design, unlike the classic structure, the active parts of the generator are not placed on the axis of the turbine, but they surround the periphery of the turbine blades and encapsulated into a protective duct. The gear of the proposed rim-driven generator is suppressed, which means fewer failures and lower maintenance issues. In addition, the proposed design simplifies the complexity of the support structure. Since the generator is submersible, no need to extend any rods to support the shaft that up to the water surface to run the generator. The addressed material cut reduces the implementation cost by reducing both material and labor costs.

Most of the WWTPs covered in this study use the typical polymeric membrane diffusers in the aeration basins. A polymeric membrane is structured as bundles of hollow fibers, which can be easily subjected to mechanical damage under the operating conditions. The polymer can be attacked by the chemicals dissolved in the wastewater. The ceramic diffusers, on the other hand, provides superior mechanical strength, since it is structured as a single piece per diffuser. It also has better chemical resistance. Although the ceramic diffusers have higher capital costs, it will be more operationally stable with less additional maintenance costs.
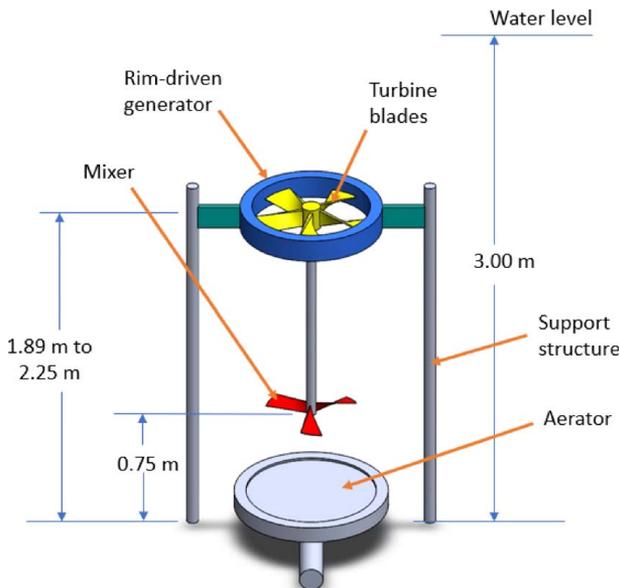
Fig. 6 Proposed turbine design

Table 1 Assessment-collected data

| Plant no.	APEC (MWh)	AAEC (MWh)	Annual electricity bill ($)	No. of aeration tanks
1	9,078.4	3,631.4	789,113	6
2	4,708.2	2,118.7	518,914	2
3	794.0	420,841.0	57,832	2
4	1,646.4	806,760.0	140,222	2
5	34,438.5	14,464.2	2,308,333	4
6	6,691.0	2,877.2	424,662	2
7	6,271.2	2,696.6	541,743	6
8	3,967.4	1,864.7	268,600	4
9	10,078.0	4,635.9	868,564	4
10	1,854.5	964,316.0	314,940	4
11	4,337.2	1,908.4	344,523	4
12	2,508.8	1,154.0	218,068	2
13	6,142.2	2,518.3	492,452	2
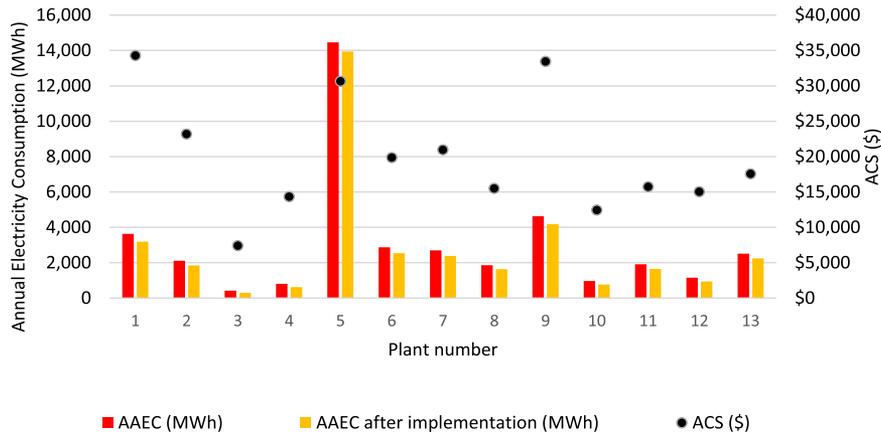
Fig. 7 Expected economic impact of the proposed project

Results

Table 1 shows the collected data for the 13 studied WWTPs, for which energy audits were performed during the period from 2017 to 2020. The annual plant electricity consumption (APEC) in megawatt-hour (MWh) and the annual plant electricity bill are calculated through the analysis applied to the monthly bills. In contrast, the annual aeration electricity consumption (AAEC) in MWh and the number of aeration tanks are collected on the day of the assessment. The table shows that the range of APEC is vast, starting from a minimum annual consumption of 794 MWh in Plant 3 to more than 34,000 MWh in Plant 5. The annual electricity bills have a wide range accordingly, with a minimum of almost $58,000 in Plant 3 to more than $2,000,000 in Plant 5. It can also be noted that the AAEC is ranging from 40% to 53% of the APEC.

Figure 7 highlights the expected impact of the current project on the 13 plants studied. On average, the AAEC after turbines installation is less than the original AAEC by 11%. The aeration annual energy-savings range from 3.6% in Plant 5 to 29.7% in Plant 3. Besides, the annual cost-savings (ACS) is calculated according to Eq. (2). ACS is almost $7,400 in Plant 3, while it reaches its maximum value of $34,300 in Plant 1.

Figure 8 demonstrates the annual energy-savings (AES) in MWh and the associated CO_2 reduction in metric tons for the 13 plants. The AES is calculated according to Eq. (1), whereas the CO_2 reduced emissions are calculated according to Eq. (5). CO_2 reduced emissions go in consonance with the AES, where both are minimum for Plant 3 (88 metric tons and 124.8 MWh), while they are maximum for Plant 5 (372 metric tons and 525.6 MWh).

Table 2 highlights the number of turbine-mixer sets proposed to be installed in each plant, and the associated economic impact expected from the current project. The number of proposed turbines is calculated based on the number of aeration tanks in each plant and the dimensions of each tank. AES % and ACS % are simply calculated according to Eqs. (3) and (4). The AES as a percentage of the APEC ranges from 1.5% in Plant 5 up to 15.7% in Plant 3. Moreover, the ACS as a percentage of the total utility bill follows the same pattern accordingly, where it ranges from 1.3% in Plant 5 to 12.8% in Plant 3.

The following set of equations were used to obtain the results shown in Tables 1 and 2:

$$AES = P \times N \times H \tag{1}$$

$$ACS = AES \times R_E + \frac{AES}{H} \times M \times R_D \tag{2}$$

$$AES \% = \frac{AES}{APEC} \tag{3}$$

$$ACS \% = \frac{ACS}{AEB} \tag{4}$$

$$CO_2 \text{ reduced emmissions} = AES \times EF \tag{5}$$

where P is the proposed microturbine-mixer set power generation (0.075 kW), N is the number of proposed microturbines to be installed in each plant, H is the plant annual operating hours (8760), R_E is the average electricity rate ($/kWh), R_D is the demand rate ($/kW), M is the months/year (12 months), AEB is the annual electricity bill ($), and EF is the emission factor (7.07×10^{-4} metric tons/kWh) [11].

Figure 9 shows the breakdown of the anticipated project implementation cost for Plant 2. It shows how the annual cost-savings
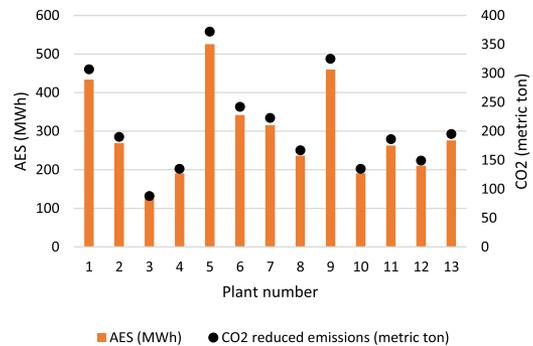

Fig. 8 Expected environmental impact of the current project

Table 2 Saving percentages due to project implementation

Plant no.	No. of turbines	AES %	ACS %
1	660	4.8	4.3
2	410	5.7	4.5
3	190	15.7	12.8
4	290	11.6	10.2
5	800	1.5	1.3
6	520	5.1	4.7
7	480	5.0	3.9
8	360	6.0	5.8
9	700	4.6	3.9
10	290	10.3	3.9
11	400	6.1	4.6
12	320	8.4	6.9
13	420	4.5	3.6
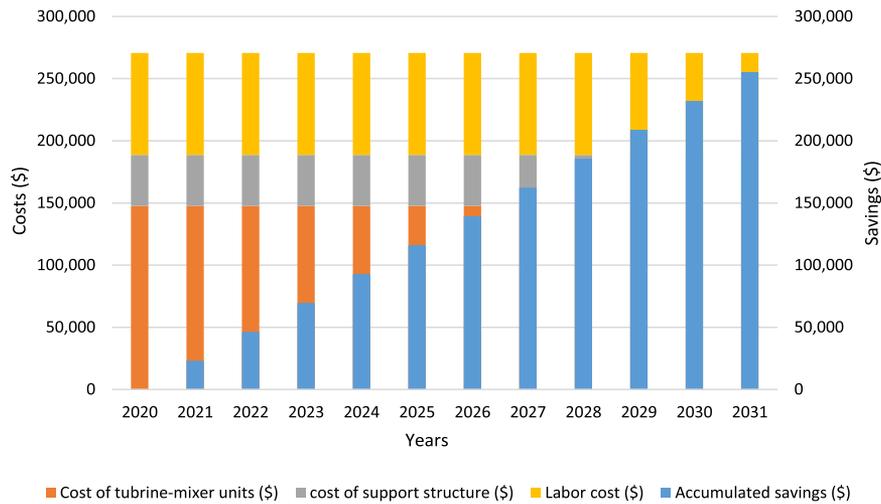
Fig. 9 Breakdown of the implementation cost and payback period for Plant 2

Table 3 Breakdown of the implementation cost and payback period for each of the studied plants

Plant no.	Cost of turbine-mixer units ($)	Cost of support structure ($)	Labor cost ($)	Implementation cost without incentives ($)	Payback period without incentives (year)	Implementation cost with incentives ($)	Payback period with incentives (year)
1	237,600	66,000	132,000	435,600	12.7	336,600	9.8
2	147,600	41,000	82,000	270,600	11.7	209,100	9.0
3	68,400	19,000	38,000	125,400	16.9	96,900	13.1
4	104,400	29,000	58,000	191,400	13.4	147,900	10.3
5	288,000	80,000	160,000	528,000	17.2	408,000	13.3
6	187,200	52,000	104,000	343,200	17.3	265,200	13.3
7	172,800	48,000	96,000	316,800	15.1	244,800	11.7
8	129,600	36,000	72,000	237,600	15.3	183,600	11.8
9	252,000	70,000	140,000	462,000	13.8	357,000	10.7
10	104,400	29,000	58,000	191,400	15.4	147,900	11.9
11	144,000	40,000	80,000	264,000	16.8	204,000	13.0
12	115,200	32,000	64,000	211,200	14.0	163,200	10.8
13	151,200	42,000	84,000	277,200	15.8	214,200	12.2

accumulate yearly to recoup the initial investment in 11 years. Therefore, by the advent of 2031, 95% of the initial investment should be returned. The average anticipated implementation cost for the 13 plants is 15 years, which is long. However, if an incentive of only $150 per single turbine is offered by utility providers, the average payback period for the 13 plants decreases to 11 years. More incentives and tax exemptions would reduce the payback period significantly, hence encouraging more plants to implement the proposed idea.

Table 3 shows the detailed breakdown of the expected implementation costs of the proposed project for the 13 plants. A turbine with a technology that fits the project, with an estimated cost of $350/unit, can be found in Ref. [24]. Commercial fan blades can perform the water column mixing job ($10 each). It is estimated that three hours ($70/hour) will be needed to install each turbine with its supporting structure. Stainless steel rods are required to build the support structure with the price and specifications shown in Ref. [25]. The payback period is the amount of time it may take for the implementation cost to be recouped. The simple payback period is calculated as follows:

$$\text{Payback period} = \frac{\text{Implementation cost ($)}}{\text{ACS ($/year)}} \qquad (6)$$

The average payback period is 15 years. However, the previous payback period can be decreased by 3 to 4 years if an incentive

of $150 per each turbine is offered by utility providers, such as Focus on Energy [26].

Conclusions

Previously, the implementation of mixers and turbines in the aeration basin of a typical WWTP was studied experimentally at the UWM Aeration Lab. Currently, turbine-mixer sets are proposed, in a modified design, to be installed on a lateral basis along the aeration tank edges above the diffuser at 25% and 63% of the water level in the tank. Based on the reported results and applying them on the 13 WWTPs covered in this study, the AES as a percentage of the APEC ranges from 1.5% up to 15.7%. The AAEC and APEC were evaluated by analyzing the plants' electricity bills and by conducting onsite energy assessments in the period between 2017 until 2020. A simple business model was also covered in this study, predicting the required number of mixer-microturbine sets, the associated implementation costs, and the simple payback periods. In addition, the associated CO_2 reduction in metric tons for the 13 plants was estimated. CO_2 reduced emissions go in consonance with the AES, where both are minimum for Plant 3 (88 metric tons and 124.8 MWh), while they are maximum for Plant 5 (372 metric tons and 525.6 MWh).

By applying the proposed microturbines to these facilities, it was demonstrated to achieve a gross annual energy-savings of 3,836.9 MWh, a gross annual cost-saving of $260,497, and total CO_2 emissions that would be reduced by 2714 metric tons/year.

Generally, the addition of the proposed microturbines can save up to 15.7% of the annual plant electricity consumption (1.3–12.8% of the plant annual electricity bills).

Risk and Challenges of Future Work

The current project might face potential challenges during experimentation, execution, and optimization. The optimum location for turbine installation needs to be determined according to experimentation in a real aeration tank, since the experimental setup at UWM lab is limited to a tank of lower height than in a plant. Moreover, the material and the diameter of the proposed turbine design needs to be decided according to the velocity of the water current in a real aeration tank as well, to make sure that the water velocity in a real situation would be able to overcome the rotor's moment of inertia. Fatigue failure is also a pivotal factor in extending the lifetime of the turbine, and the entire structure, surface finish treatment parameters require many tests to determine the suitable surface roughness. This will ensure more effective protection of the turbine and the entire system parts from the impact of any dissolved chemicals and particles in the wastewater. In addition, a proper hydrophobic coating is needed to eliminate any scaling, particles, and algae interaction, since turbine parts and membrane will be susceptible to these contaminants during the entire operation time. The coating will add more weight to the whole system. Therefore, the effect of the coating on the turbine performance should be optimized.

References

[1] Hasan, A., ElGammal, T., Amano, R., and Khalil, E., 2018, "Flow Patterns and Temperature Distribution in an Underground Metro Station," Proceeding of 12th ASME International Conference on Energy Sustainability, Lake Buena Vista, FL, June 24–28.

[2] Hasan, A., Jackson, R., and Amano, R., 2019, "Experimental Study of the Wake Regions in Wind Farms," ASME J. Energy Resour. Technol., **141**(5), p. 051209.

[3] Hasan, A., ElGammal, T., Jackson, R., and Amano, R., 2020, "Comparative Study of the Inline Configuration Wind Farm," ASME J. Energy Resour. Technol., **142**(6), p. 061302.

[4] Hasan, A., Abousabae, M., Salem, A., and Amano, R., 2020, "Study of Aerodynamic Performance[Q5] and Power Output for Residential-Scale Wind Turbines," ASME J. Energy Resour. Technol., **143**(1), p. 011302.

[5] Pawlak-Kruczek, H., Urbanowska, A., Yang, W., Brem, G., Magdziarz, A., Seruga, P., Niedzwiecki, L., Pozarlik, A., Mlonka-Medrala, A., Kabsck-Korbutowicz, M., Bramer, E., Baranowski, M., Sieradzka, M., and Tkaczuk-Serafin, M., 2020, "Industrial Process Description for the Recovery of Agricultural Water From Digestate," ASME J. Energy Resour. Technol., **142**(7), p. 070917.

[6] Abbas, A., Saravani, M., Al Haddad, M., Qandil, M., and Amano, R., 2018, "A Comparative Study of Industrial Energy Assessments," Proceeding of 12th ASME International Conference on Energy Sustainability, Lake Buena Vista, FL, June 24–28.

[7] Abdelhadi, A., Salem, A., Abbas, A., Qandil, M., and Amano, R., 2019, "Study of Industrial Energy Assessments for Different Sectors," AIAA Propulsion and Energy 2019 Forum, Indianapolis, IN, Aug. 19–22.

[8] Giacone, E., Manco, S., and Gabriele, P., 2008, "Energy Management Techniques for Small- and Medium Size Companies," ASME J. Energy Resour. Technol., **130**(1), p. 012002.

[9] Nourin, F., Abbas, A., Qandil, M., and Amano, R., 2020, "Analytical Study to Use the Excess Digester Gas of Wastewater Treatment Plants," ASME J. Energy Resour. Technol., **143**(1), p. 012104.

[10] Amano, R., Abbas, A., Al Haddad, M., and Qandil, M., 2019, "Energy Consumption, Energy-Saving and Emissions Reduction of Wastewater Treatment Plants (WWTPs) in Wisconsin," AIAA Propulsion and Energy 2019 Forum, Indianapolis, IN, Aug. 19–22.

[11] "Energy and the Environment," United States Environmental Protection Agency, https://www.epa.gov/energy/greenhouse-gases-equivalencies-calculator-calculations-and-references, Accessed June 29, 2020.

[12] Abbas, A., Qandil, M., Al Haddad, M., Saravani, M., and Amano, R., 2019, "Utilization of Hydro-turbines in Wastewater Treatment Plants," ASME J. Energy Resour. Technol., **141**(6), p. 062011.

[13] Abbas, A., Qandil, M., Al Haddad, M., and Amano, R., 2020, "Investigation of Micro Kaplan Hydro-turbine Performance Using Multi-disciplinary Optimization," ASME J. Energy Resour. Technol., **142**(5), p. 052101.

[14] "Water and Wastewater Treatment Energy Savings Guide," Energy Trust of Oregon, Portland, OR, 2017.

[15] "Water & Wastewater Industry Energy Best Practices Guidebook," Wisconsin Focus on Energy, 2020.

[16] Alkhalidi, A., and Amano, R., 2015, "Factors Affecting Fine Bubble Creation and Bubble Size for Activated Sludge," Water Environ., **29**(1), pp. 105–113.

[17] Alkhalidi, A., Amano, R., and Khawaja, M., 2019, "Estimation Model of KLa Constant Using Bubble Release Rate and Bubble Size," Sch. J. Eng. Tech., **7**(2), pp. 33–40.

[18] Alkhafaji, A., Alkhalidi, A., and Amano, R., 2016, "Effect of Water Column Height on the Aeration Efficiency Using Pulsating Airflow," Jordan J. Mech. Ind. Eng., **10**(2), pp. 45–50.

[19] Alkhalidi, A., Al Ba'ba'a, H., and Amano, R., 2016, "Wave Generation in Subsurface Aeration System: A New Approach to Enhance Mixing in Aeration Tank in Wastewater Treatment," Desalin. Water Treat., **57**(56), pp. 27144–27151.

[20] Amano, R., and Alkhafaji, A., 2020, "Evaluation of Ceramic and Membrane Diffusers Under Different Water Columns With Pulsating Air Flow Method," Int. J. Energy Clean Environ., **21**(2), pp. 145–167.

[21] Al Ba'ba'a, H., and Amano, R., 2017, "A Study of Optimum Aeration Efficiency of a Lab Scale Air-Diffused System," Water Environ., **31**(3), pp. 432–439.

[22] Alkhalidi, A., Bryar, P., and Amano, R., 2016, "Improving Mixing in Water Aeration Tanks Using Innovative Self-powered Mixer and Power Reclamation From Aeration Tank," Jordan J. Mech. Ind. Eng., **10**(3), pp. 211–214.

[23] Amano, R., and Alkhalidi, A. "Membrane for Air Diffusers". Milwaukee, WI, US Patent No. 2013/0099401, April 25, 2013.

[24] Water Lily, https://shop.waterlilyturbine.com/products/waterlily-turbine?variant=29523372048445, Accessed June 29, 2020.

[25] Mid-west Steel Supply, https://www.midweststeelsupply.com/store/304stainless steelroundbar, Accessed May 30, 2020.

[26] Focus on Energy, https://focusonenergy.com/business#program-catalogs-applications, Accessed June 29, 2020.